Scientific Reports

https://doi.org/10.1038/s41598-026-63594-w

Article in Press

Impact of nitrogen deposition and critical load exceedances on India's ecologically sensitive regions

Received: 10 March 2026

Accepted: 20 July 2026

Published online: 12 August 2026

Cite this article as: Shende P., Pawar P.V., Sutton M.A. *et al.* Impact of nitrogen deposition and critical load exceedances on India's ecologically sensitive regions. *Sci Rep* (2026). https://doi.org/10.1038/s41598-026-63594-w

Pritanjali Shende, Pooja V. Pawar, Mark A. Sutton, Rama Krishna Karumuri, Gaurav Govardhan & Sachin D. Ghude

Impact of Nitrogen Deposition and Critical Load Exceedances on India's Ecologically Sensitive Regions

Pritanjali Shende[1], Pooja V. Pawar[1*], Mark A. Sutton[2], Rama Krishna Karumuri, Gaurav Govardhan[1] and Sachin D. Ghude[1*]

[1] Indian Institute of Tropical Meteorology (IITM), Ministry of Earth Sciences, Pune, India

[2] UK Centre for Ecology & Hydrology (UKCEH), Edinburgh, UK.

Corresponding author: Pooja V. Pawar (email: pooja.pawar@tropmet.res.in; sachinghude@tropmet.res.in)

Abstract

Human-induced nitrogen (N) deposition poses a serious threat to biodiversity in ecologically sensitive protected areas. India, a major hotspot of reactive nitrogen (N*r*) emissions, has so far lacked high-resolution assessments of nitrogen deposition impacts over its national parks (NPs). This study presents the first high-resolution modelling of total nitrogen deposition over India using an updated ammonia (NH_3) emission inventory, which remains subject to substantial uncertainty. Ecological risks were evaluated under a baseline scenario (BS-2015) and a future emission scenario (FES-2030) by comparing simulated deposition with critical load (CL) thresholds prescribed for ecosystems in the United States (USA), China, and Europe. Under BS-2015, 6, 12 and 18 NPs already exceeded China, Europe and USA CL values, respectively, whereas under FES-2030, the number of NPs CL exceedances doubled, with 25 NPs exceeding USA CLs and 12 exceeding European CLs. The exceedances of Chinese CLs were less frequent, but a relative increase in the total N deposition ranging from 5% to 124% were projected across the various ecosystems. The findings indicate increasing N stress through 2030 and highlight the need for long-term field studies to establish region-specific critical load thresholds for India.

Keywords: WRF-Chem, Nitrogen deposition, India, national parks, critical load exceedance

Introduction

Anthropogenic alteration of the global nitrogen (N) cycle represents one of the most profound environmental changes during industrialization. These changes are majorly driven by the industrial Haber-Bosch process, that converts inert atmospheric dinitrogen (N_2) into reactive nitrogen (N_r) species [1]. About half of the world's population depends on this invention for their food security;

however, the unintentional release of N_r into the environment leads to a series of negative consequences not only on human health but also on the various sensitive ecosystems causing detrimental effects on nature [2]. The atmospheric N deposition of N_r species (NO, NO_2, HNO_3, peroxyacetyl nitrate -PAN, NH_3, NH_4^+) occurs when emitted N oxides ($NO_x = NO + NO_2$; emitted by fossil fuel combustion, transportation, industrial, residential or other sources) and ammonia (NH_3 ; emitted from agricultural and livestock activities) chemically transform and ultimately get deposited in the terrestrial and aquatic ecosystems through wet and dry deposition processes [3]. N deposition in an ecosystem, leads to plant growth, carbon sink and promotes crop yield [4,5], whereas excessive N deposition causes soil and water acidification [6], leaching of base cations [7,8] and disrupts the flux of key greenhouse gases (N_2O)[9], reduces soil buffering capacity [10], eutrophication and biodiversity loss in nutrient-poor ecosystems [11] and also affects human health [12]. High N_r loading impacts the atmospheric chemistry as (i) they are the precursors for the formation of secondary inorganic aerosols (SIA) such as ammonium chloride (NH_4Cl), ammonium sulfate $(NH_4)_2SO_4$) and ammonium nitrate (NH_4NO_3)) [13,14], which indirectly harms human health [15] and, (ii) actively participates in tropospheric ozone (O_3) formation and chemistry [16].

North America and Europe have established an extensive monitoring network (e.g., NADN, EMEP) and implemented successful regulatory frameworks to curb emissions of NO_x and NH_3 to reduce the adverse impact of these N_r on ecological and human health [17]. The rise in the atmospheric deposition of N_r in the sensitive zones would lead to a permanent loss in the biodiversity of such regions and would ultimately lead to the change in the plant composition subsequently affecting the biodiversity of that ecosystem [18–20]. The N deposition value above which there is a loss, damage or changes in the behaviour, physiology or composition of the plant diversity in an ecosystem is called the critical load (CL) for that particular sensitive species [18]. Various and detailed critical load studies have been conducted by the USA, Europe and China to protect the ecologically sensitive zones of these countries [19–21].

India has a vast ecological wealth with a huge biodiversity of 7-8% of documented species and 47,000 reported plant species [22]. The 104 NPs (SI-Table S1, SI-Figure S1) of India encompasses around one-fifth of the nation's territory with diverse ecosystems like alpine/sub-alpine, desert, mangrove, deciduous, evergreen/semi-evergreen forests [23]. The NPs in India are designated as IUCN Category-II protected areas with 4 among 34 global biodiversity hotspots [24]. The vulnerability of these ecosystems to atmospheric N deposition been neglected and the major studies have focused on the effect of N pollution in the urban areas, fertilization application, livestock N emissions, agricultural practises and eutrophication from the runoff without addressing the N deposition processes and their effect on the vegetation and various ecosystems [25–27]. India presents a critical and rapidly intensifying N_r pollution hotspot [28]. It is the second-largest consumer and third-largest producer of fertilizers globally, with highest urea production of 31.4 million metric tonnes for the financial year 2023-24 [29]. The agricultural activities including livestock emissions are the paramount source of atmospheric NH_3 emissions [30]. Simultaneously, a rapidly expanding industrial sector, coal-fired power plants, and transportation sector contribute significantly to NO_x emissions [31]. The Indo-Gangetic Plain (IGP) region of India is known as the global epicentre for NH_3 concentration [13] and N_r deposition [28], with estimated fluxes often exceeding critical loads (> 10-15 kg N ha^{-1} yr^{-1}) known to cause ecological harm [30,32].

Several studies have assessed nitrogen deposition across India [32–50]; however, experimental investigations into critical load exceedance remain limited [47] and have not yet been conducted for ecologically sensitive zones. Long-term assessments of atmospheric nitrogen deposition over the Indian subcontinent are also scarce [47]. GEOS-Chem modelled Nr deposition, using Representative Concentration Pathways) RCP/MIX emissions (Asian anthropogenic emissions inventory) from 2010 till 2100, over the ecologically sensitive zones of India presented the need to carry N deposition studies as more than 80 NPs among 104 exceeded the critical load exceedance values of >10kg-N ha^{-1} a^{-1} [32]. A substantial uncertainty persists in the Indian nitrogen budget [51] due to limitations in emission inventories and the lack of nationwide observational constraints and atmospheric deposition monitoring networks [20–26,52]. Previous national-scale assessments have largely relied on global chemical transport models and global emission inventories, which are subject to uncertainties arising from gaps in sector-specific activity data, emission factor selection, and methodological inconsistencies challenges that are particularly pronounced in low- and middle-income countries such as India. The use of a 35 km × 35 km (WRF-Chem) regional modeling framework provides a detailed representation of spatial variability in emissions, meteorology, and nitrogen deposition across India. Such spatial detail facilitates the identification of localized deposition hotspots and critical load exceedances that may be less resolved in coarser-resolution global model simulations, although a direct model comparison is beyond the scope of this study (SI-Figure S1). We quantify the present for the year

2015 and the future for the year 2030, atmospheric nitrogen deposition over India's NPs. The model is driven by an updated, India-specific NH_3 emission inventory developed under the South Asian Nitrogen Hub (SANH) [53], incorporating refined data on fertilizer use, crop distribution, livestock populations, and region-specific emission factors. Nitrogen deposition is evaluated across major ecosystem types under baseline (2015; BS-2015) and future (2030; FES-2030) emission scenarios. We evaluate whether improvements in modelled nitrogen deposition enhanced the assessment of ecosystem CL exceedance based on internationally reported thresholds [11,19,20], recognizing that ecological impacts may occur even at lower deposition levels. Given the uncertainty in ecosystem recovery, this study provides more robust and realistic estimates of nitrogen deposition risks over India's ecologically sensitive regions, enabled using updated emission inventories.

Results

Model evaluation

The modelled deposition fields are compared with the ground-based deposition and concentration values from multiple observational studies carried out across India (as shown in SI-Table – S2(i) and SI-Table – S2(ii) and SI-Figure S3) to evaluate the model's ability to reproduce observed magnitudes and regional variability. Normalized mean bias (NMB) and correlation coefficients are determined as explained in SI-section S1. Figure1 presents that the modelled wet deposition of NH_4^+ is underestimated with NMB as -0.31 and the correlation coefficient is observed to be 0.50. The modelled nitrate (NO_3^-) wet deposition flux is observed to be in consistent with the observation values with NMB and correlation coefficient as 0.74 and 0.85 respectively. Overall, these small biases suggest that the model reproduces the mean wet N deposition reasonably well. Despite the strong correlation, the model over-predicts NO_3^- wet deposition, and from a quantitative perspective. Overall, the model demonstrates a reasonable skill in reproducing observed wet deposition patterns. It should be noted that the wet deposition observations used for model evaluation were collected during 1991–2008, compared to BS-2015. This temporal mismatch reflects the limited availability of long-term measurements of wet N deposition parameters in India. Consequently, the evaluation is intended to assess the model's ability to reproduce the broader spatial distribution and its magnitude. A definitive validation will be considered in future work. Furthermore, NH_3 and NO_x emissions in India have changed substantially over recent decades, with NH_3 emissions estimated to have increased by approximately 1.8% yr^{-1} and NO_x emissions by approximately 7% yr^{-1}, driven by rapid economic development and increasing anthropogenic activities [51,54]. Therefore, the observed historical emission trends represent an important source of uncertainty in comparing observations and the 2015 simulations. Since NO_3^- and NH_4^+ aerosols are key contributors to the N deposition, we further evaluated the simulated NO_3^- and NH_4^+ concentrations against observations in the Fig SI-Figure S3. Modelled NO_3^- and NH_4^+ concentrations had a correlation coefficient of 0.7 and 0.9 and a NMB of 1.2 and -0.06 respectively. It is observed that the NO_3^- aerosols are highly overestimated in the model while ammonium is near neutral. The model captures the spatiotemporal variability of NH_4^+ well ($r = 0.9$), while the lower correlation for NO_3^- ($r = 0.7$) suggests greater uncertainty in simulating NO_3^-. These discrepancies may be associated with uncertainties in NO_x emissions and gas-to-particle partitioning influencing the nitrate formation [14].

We further evaluated the model performance by comparing the simulated total NH_3 and NO_2 column densities (molecules cm^{-2}) with satellite observations from the Infrared Atmospheric Sounding Interferometer (IASI) and Ozone Monitoring Instrument (OMI), respectively, to assess the model's accuracy (Figure 2). The simulated total column ranges of NH_3 and NO_x are consistent with those reported in previous studies, providing confidence in the model's representation of these atmospheric species [13,55]. The model captures the spatiotemporal variability of NH_3 particularly well ($r = 0.90$) (Figure 2a). Although the correlation coefficient for NO_2 is slightly lower ($r = 0.82$), it still indicates that the model is able to capture the spatial distribution and major emission hotspots with good accuracy (Figure 2b). However, the NMB values for NH_3 and NO_2 are -0.39 and 2.10, respectively, indicating that the model underestimates the mean NH_3 total column while substantially overestimating the mean NO_2 column. The NMB for NH_4^+ wet deposition is also negative (-0.31), indicating the ammonia-rich environment over the IGP. Furthermore, the comparison with IASI observations shows that the model still overestimates NH_3 over the IGP despite the negative bias (Figure 2a). Thus, underestimation of NH_4^+ wet deposition may also be influenced by uncertainties in HCl emissions [14]; however, quantifying this effect requires dedicated sensitivity simulations and will be investigated in future work. In contrast, the slight overestimation of NO_3^- wet deposition and NO_2 suggests that the model captures the overall high-NO_x environment over the study region, although the magnitude of NO_2 is overestimated. Overall, compared with previous studies, the model demonstrates improved performance, with comparatively lower bias in NH_3 simulations [13,56]. Here, we primarily assess the model's ability to reproduce the overall spatial distribution and magnitude of the simulated species A detailed analysis of the model–observation discrepancies is beyond the scope of this study and warrants future work. Nevertheless, while satellite observations provide an independent evaluation of the simulated NH_3 and NO_2 column distributions, the validation of aerosol concentrations and N deposition remains constrained by the limited availability of contemporaneous ground-based observations. This underscores the need for long-term, continuous monitoring of atmospheric composition and N deposition to further improve and validate model simulations. The modelled total N wet (1.8 Tg-N a^{-1}) and dry (1.5 Tg-N a^{-1}) deposition values over India are well matched with the observation values given by Kulshreshtha (2017), 1.97 Tg a^{-1} and 1.67 Tg-N a^{-1} respectively [28].

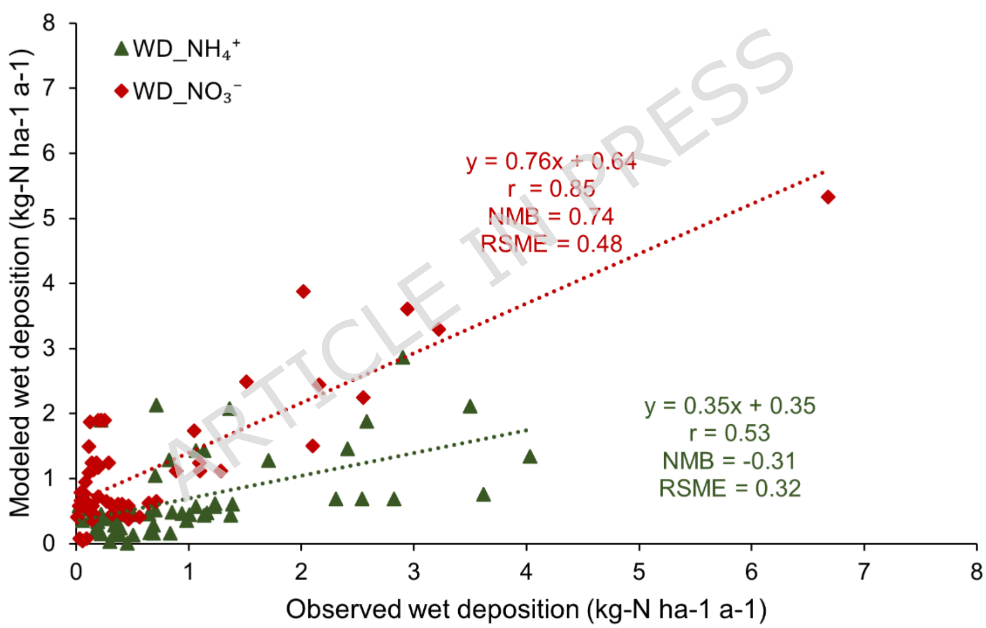

Figure1: Comparison of model results with ground-based observations reported in studies conducted across India.

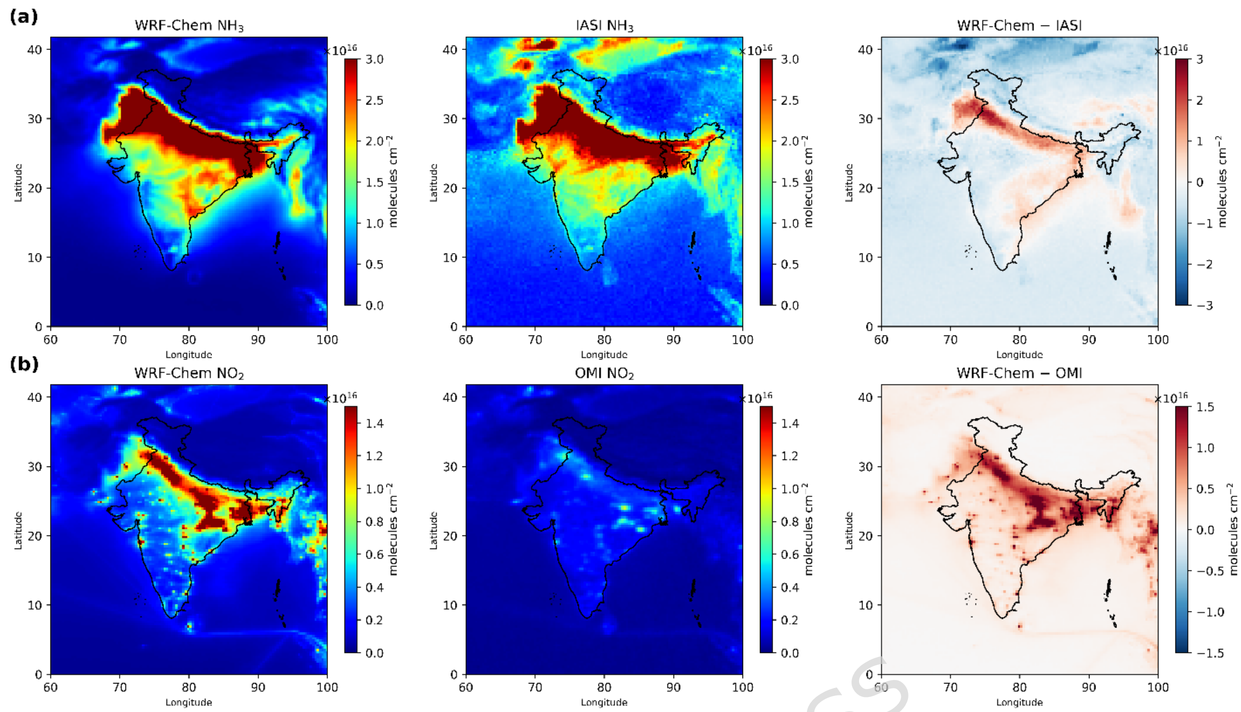

Figure2: Comparison of simulated and satellite-derived total (a) NH_3 and (b) NO_2 column (molecules cm^2) over India.

Nitrogen deposition over India

Figure3 shows the spatial representation of oxidized (NOy = HNO_3, HNO_4, NO, NO_2 and NO_3), reduced (NH_x = NH_3 and NH_4) and total N*r* deposition (NO_y+NH_x) over India for BS-2015 and FES-2030 scenario. The BS-2015 deposition of NH_x and NO_y is 2.94 Tg-N a^{-1} and 0.33 Tg-N a^{-1}, and for the FES-2030 it was observed to be 3.81 Tg-N a^{-1} and 0.99 Tg-N a^{-1} respectively. The total N*r* deposition over India is estimated as 3.2 Tg-N a^{-1} and 4.7 Tg-N a^{-1} for the BS-2015 and FES-2030, respectively. A detailed N deposition processes are explained in SI-Table S3. The total N*r* deposition values during the FES-2030 are 1.5 times higher than the BS-2015 total Nr depositions. The relative change in the total N deposition with respect to BS-2015 in the states like Maharashtra, Goa, Daman and Dui, Chhattisgarh, Odisha, Madhya Pradesh, Karnataka, Andhra Pradesh, Telangana, Haryana, Uttar Pradesh and Rajasthan was observed to be greater than 50% as can be seen from SI-Table S4. These states constitute of 40 ecologically sensitive zones and with a potential rise in the N loading and deposition in these regions would adversely affect their ecosystems. A detailed N deposition assessment in BS-2015 and FES-2030 scenarios is performed below to observe the CL exceedance occurred in the sensitive areas and their possibility of change with respect to BS-2015.

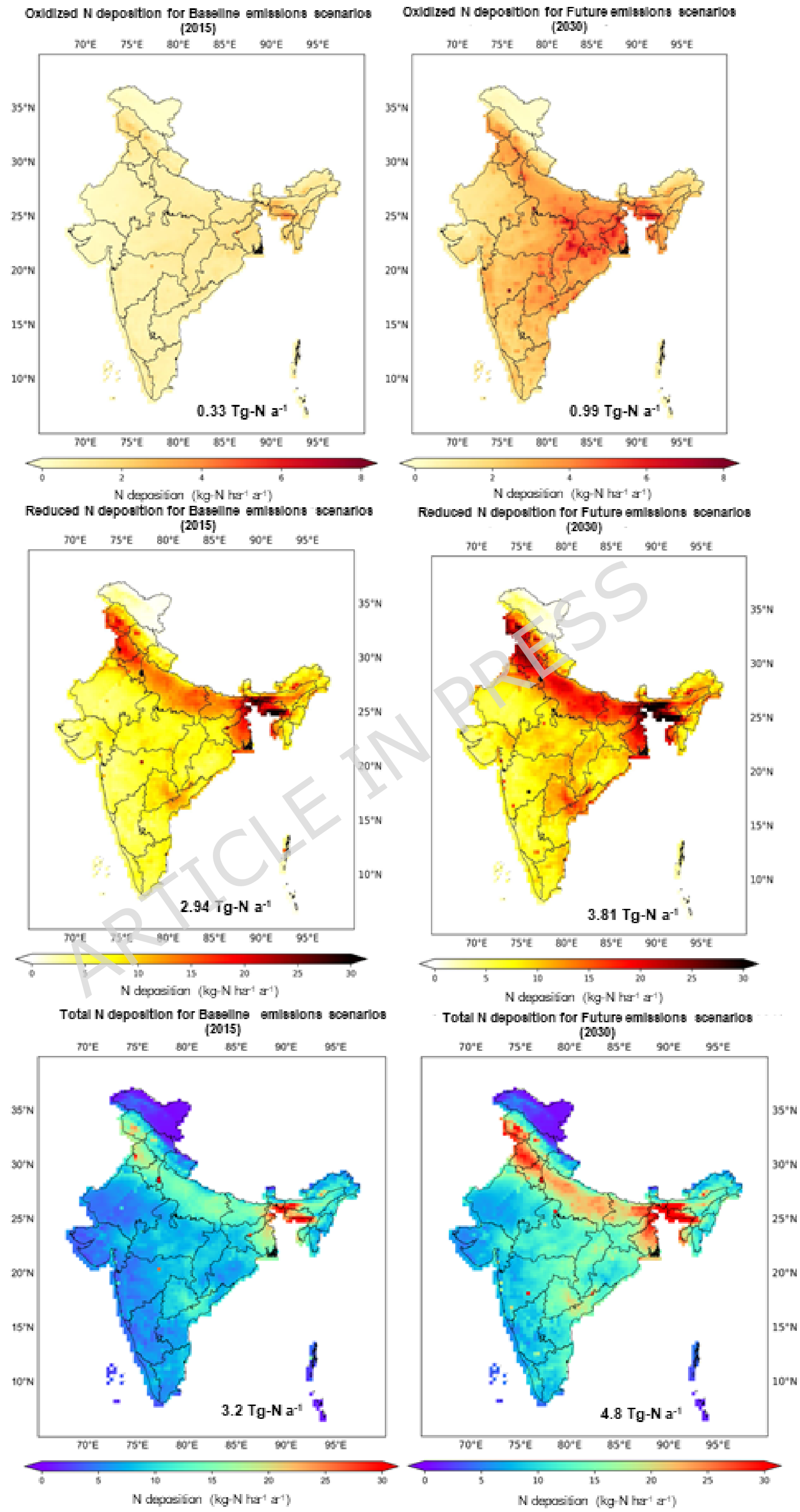

Figure3: Spatial oxidized, reduced and total N deposition for the BS-2015 and FES-2030 over India.

Nitrogen deposition in the National parks of India

Figure4 presents the total N*r* deposition in the NPs of India under BS-2015 and FES-2030 scenarios respectively. SI-Figure S4 presents the relative change in the total N*r* deposition with respect to BS-2015 scenario for all the NPs of India. The range of critical load exceedance values from USA, China and Europe obtained from various studies are shown in Table1 in the Methods section. A significant rise in the number of NPs is observed exceeding the CL values in the FES-2030 scenario. A detailed explanation about the N deposition in various ecosystems is provided below with respect to their CL exceedance values.

Alpine ecosystem: The total N deposition values in BS-2015 scenario ranged from 0.53 kg-N ha^{-1} a^{-1} (Neora valley NP) to 19.4 kg-N ha^{-1} a^{-1} (Kishtawar NP). 12 out of 15 NPs in the alpine ecosystem exceeded the USA CL exceedance values. 5NPs exceed the Europe CL values while none exceeded China CL values. In the FES-2030 scenario 12 NPs exceeded USA and Europe's CL value while none exceeded China CL exceedance values. The Model predicted that NPs like Kanchanzonga, Mouling and Neora valley NP had <1 kg-N ha^{-1} a^{-1} of total N deposition in both the scenarios. The relative changes are observed to be as low as 21% (Neora valley NP) and as high as 57% (Valley of flowers). A positive relative change is expected in a time span of 15 years where 80% of alpine ecosystems will be affected with the N deposition fluxes. According to the past studies reported in the USA for the sensitive zones in the alpine meadows of California presented a shift in the biodiversity community or change in the species composition [21] at a very low level of N deposition [20]. Hence, in the ecologically sensitive zones of the alpine ecosystem's conservation is much of a concern for protecting the biodiverse and sensitive species.

Mangrove ecosystem: Bhitarkanika NP exceeded the CL values for USA in both the scenarios and none exceeded the China CL values. There are no exceedance values prescribed by Europe for the mangrove ecosystem. A maximum of 28 kg-N ha^{-1} a^{-1} of N deposition in the FES-2030 scenario with a leap from 17.4 kg-N ha^{-1} a^{-1} in the BS-2015 scenario is observed. Even though the values do not seem to exceed the China critical load exceedance values for mangrove ecosystem, still a strong percentage of changes (20% - 60%) could lead to carbon sink [57], prominent changes [58,59] and loss in the plant community [60] along with eutrophication, production of toxic bloom algae [61–63], enhanced microbial activity, changes in the biogeochemistry [64,65] and also NO_3^-

leaching [66]. India lacks N deposition study for the mangroves. The critical load estimations would require understanding the responses of various components of the ecosystem towards N deposition as they can be the indicators for the ecological harm [20].

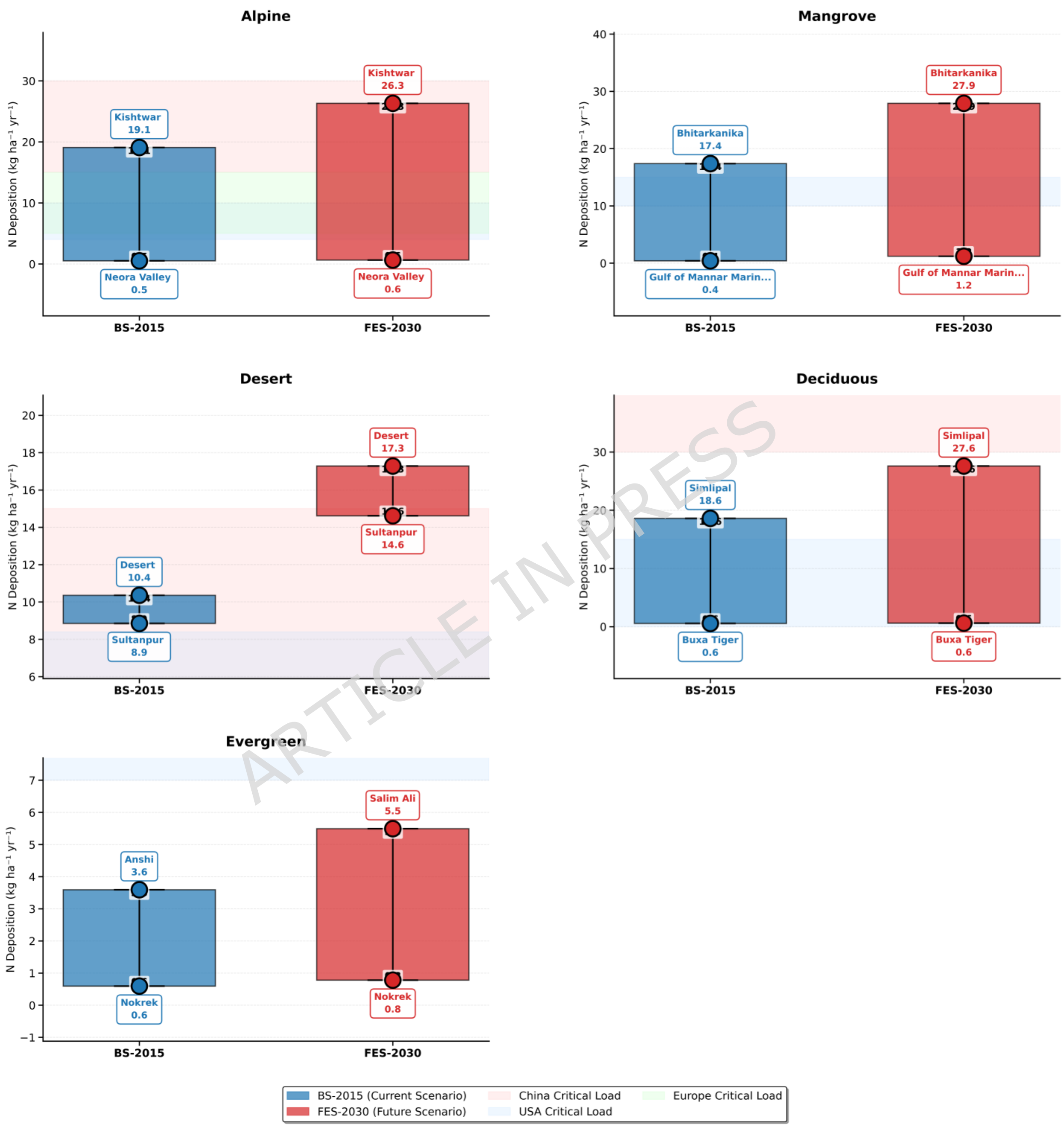

Figure4: Total N deposition (kg-N ha^{-1} a^{-1}) in ecologically sensitive zones of India under the BS- 2015 (blue colour bar) and FES-2030 (red colour bar) containing the minimum and the maximum total N deposition for specific ecosystems of India along with the NP name. The background blue colour represents the USA CL limits, green (in the alpine region) represents the Europe CL limits and the red colour band is the China CL limits.

Desert ecosystem: There are two NPs in this ecosystem: Desert NP and Sultanpur NP. Both exceeded the CL exceedance values of USA in both the scenarios (BS-2015 and FES-2030). Desert NP (17.6 kg-N ha^{-1} a^{-1}) exceeded China CL values in FES-2030 scenario, but none exceeded the CL exceedance in BS-2015 scenario. Desert ecosystems are low-biomass regions due to dry and hearted climates [20], any increment in the N loading would lead to growth of invasive species [62]. This irreversible change in plant diversity like introduction of new species in the ecosystem indirectly affects the plant community already present in the ecosystem.

Deciduous ecosystem: It is observed that none of the NPs exceeded the China CL values whereas Rajaji NP (15.2 kg-N ha^{-1} a^{-1}) and Shimlipal NP (18.6 kg-N ha^{-1} a^{-1}) exceeded USA CL values of 15 kg-N ha^{-1} a^{-1}. 6NP exceeded the USA CL values in the FES-2030 scenario. A relative change of 5% - 85% is observed in this ecosystem. Deciduous ecosystems are diverse in plant physiology and are around 65.6% of the total forest area of the Indian subcontinent. Any addition of N nutrients in the ecosystem would lead to an enhanced soil acidification [67], and NO_3^- leaching [19,68]. This ultimately reduces the soil fauna diversity [69] because of N deposition mediated acidification and not fertilization .

Evergreen ecosystem: None have exceeded China and USA CL values for both the scenarios. The relative change in the total deposition was estimated as 15% - 124%. These ecosystems are N limited regions and hence, not much change in the biodiversity could be seen because of higher CL values.

Overall 6, 12 and 18 of the total NPs of India exceeded China, Europe and USA CL values in BS-2015 and 12, 12 and 25 NPs exceeded the CL values of China, Europe and USA respectively in the FES-2030 scenario. The FES-2030 scenario used in this study is based on the ECLIPSE v4 Maximum Feasible Reduction (MFR) scenario, in which the growth in livestock numbers (approximately 1–2% yr^{-1}) is largely offset by NH_3 emission mitigation measures, resulting in relatively stable NH_3 emissions between 2015 and 2030. In contrast, NO_x emissions increase more rapidly (approximately 7% yr^{-1}), consistent with continued growth in anthropogenic activities [51,70,71]. More recent ECLIPSE v6 Current Legislation (CLE) projections without additional NH_3 abatement indicate an approximately 23% increase in NH_3 emissions over India between 2015 and 2030 [72]. Therefore, to assess the uncertainty associated with future NH_3 emissions, a first-order sensitivity analysis is performed using ±30% NH_3 emission perturbations. Assuming an approximately linear response of NH_x deposition to moderate emission changes [13,73–75], the baseline deposition fields are scaled by factors of 0.7 and 1.3 (SI-Figure S5). The mean NH_x deposition varied from 2.08 to 3.85 kg N ha^{-1} yr^{-1} under the -30% and +30% emission scenarios, respectively. While the deposition magnitude changed, the spatial pattern of critical load exceedance and the number of national parks exceeding critical loads remained largely unchanged. This is because the resulting total N deposition (~2.0 and ~4.8 kg N ha^{-1} yr^{-1} for the -30% and +30% scenarios, respectively) is comparable to that simulated under the BS-2015 and FES-2030 scenarios. Furthermore, a comparison of total N deposition simulated by WRF-Chem and GEOS-Chem (SI-Figure S2) shows that, although GEOS-Chem generally estimates higher deposition than WRF-Chem, both positive and negative point-wise differences are evident across national parks and ecosystem types [32]. This suggests that while the absolute magnitude of deposition is model dependent, the overall spatial patterns and assessment of vulnerable ecosystems remain broadly consistent. It has been observed that the total N deposition in these ecologically sensitive zones will rise till 2030 and due course of action is needed to undergo long term field studies to generate India's CL exceedance values for the ecologically sensitive zones of India. This will further be useful for monitoring the sensitive species in these zones and preserving the biodiversity of the country.

Furthermore, considering the 2030 predictions, there is a need to conduct long-term experimental research on how N deposition alters biodiversity in these ecologically sensitive areas. This work urges to establish a range of critical load thresholds for the various vulnerable species through the long-term N deposition studies.

Discussion

The current work focuses on assessing the impact of using a newly developed ammonia emission inventory based on actual activity statistics and the future trajectories of N deposition across various NPs in India. Despite the inherent uncertainties, the newly developed ammonia emission inventory demonstrates an improved performance and yields robust spatial patterns of N deposition. This underscores the need for generating region and ecosystem specific CL values for India.

Under the FES-2030 scenario, a substantial increase in N deposition is projected for several NPs, along with a rise in the number of NPs exceeding CL thresholds prescribed for ecosystems in China, Europe and USA. These exceedances suggest severe and ecosystem-specific ecological implications. Alpine, mangrove, and desert ecosystems are identified as being at risk, with projected nitrogen (N) loads likely to drive biodiversity shifts, soil acidification, the proliferation of invasive species, and fundamental alterations in biogeochemical cycles, including a potential weakening of the carbon sink capacity of mangroves. Although evergreen forests currently exhibit lower CL exceedances due to their higher nitrogen tolerance, the large relative increases in deposition (up to 124%) warrant immediate attention. The absence of region-specific and species-specific CL values further complicates impact assessments and necessitates reliance on international benchmarks. As these CL values vary substantially (~ threefold between USA and China) across the same ecosystem type. This could be due to the differences in the soil type, climatic conditions and species composition. Our reliance on USA, China and Europe benchmarks states that the reported exceedances are to be considered qualitative indicators rather than the quantitative thresholds. For Indian ecosystems the CL values for the dry desert and the N sensitive Himalayan alpine could be lower or higher than the nitrogen deposition CL values prescribed by USA, China and Europe. But this limitation amplifies the urgent necessity of developing India's own ecosystem specific CL values through long-term N deposition field experiments in these ecologically sensitive zones. Beyond these direct terrestrial impacts, atmospheric N deposition also poses an indirect threat to surface water bodies within and downstream of protected areas. Feng et al. (2024) [76] demonstrated that 77–99% of N inputs to rivers from atmospheric N deposition occur not through its direct deposition onto water surfaces, but through the transport of deposited N from terrestrial landscapes into aquatic ecosystems. This indirect pathway significantly contributed to eutrophication in Chinese river basins, particularly as agricultural NH_3 emissions became the dominant source of total N deposition. For India's protected wetlands and lakes including Ramsar sites such as Chilika Lake, Keoladeo National Park, and Loktak Lake a similar process is likely to take place. Atmospheric N deposition onto surrounding forest, grassland, or agricultural land can be leached or eroded into these water bodies, exacerbating eutrophication, algal blooms, and hypoxia even when direct deposition onto the water surface is modest. Given that several Indian protected areas already face nutrient pollution pressures, ignoring this indirect pathway risks substantially underestimating the full ecological footprint of N deposition on aquatic biodiversity and water quality.

The findings therefore serve as an urgent call to action. To effectively preserve these ecologically sensitive regions, India must prioritize the development of nationally relevant critical load exceedance standards through long-term field observations and ecosystem-level studies. This is a crucial prerequisite for reliable ecological monitoring, protection of sensitive species from the escalating threat of nitrogen deposition. However, reducing nitrogen deposition itself particularly the agricultural NH_3 emissions that drive much of the threat requires practical, scalable intervention strategies. A demonstration square approach was successfully implemented in North China Plain to mitigate cropland NH_3 emissions while maintaining high cereal production. In Quzhou County, this coordinated campaign involving government, researchers, businesses, and smallholder farmers achieved a 49% and 39% reduction in the amount of NH_3 gas lost from fertilizer applied to fields of wheat and maize, respectively, with concurrent increase in nitrogen-use efficiency (percentage of applied nitrogen fertilizer that is actually taken up by the crop) by 28–40% and farmers profitability by 19–25%, and a 40% reduction in the atmospheric NH_3 concentration at the county scale [77]. This approach demonstrated feasibility of source-level NH_3 mitigation at meaningful scales and also, a replicable blueprint: coordinated, multi-stakeholder intervention at the county level can achieve large NH_3 reductions without compromising food production or farmer livelihoods. For India, where agricultural NH_3 emissions constitute a substantial fraction of total N deposition, reducing emissions from upwind agricultural districts in states such as Punjab, Haryana, Uttar Pradesh, Andhra Pradesh would, by mass balance principles, lower NH_x deposition to downwind national parks, wetlands, and alpine zones. Such an integrated approach combining source mitigation with ecological monitoring offers a concrete pathway toward reducing the nitrogen deposition threats projected under our FES-2030 scenario. As a result for India, future research should couple demonstration-square emission reductions with chemical transport models (WRF-Chem) to estimate the source-receptor relationship between agricultural districts and specific national parks as an essential step before scaling such interventions for ecosystem protection.

Methods

Emissions

Anthropogenic NH_3 emissions are obtained from a newly developed bottom-up inventory produced under the South Asian Nitrogen Hub (SANH) [53], Global HCl emissions are taken from the dataset provided by Zhang et al, 2022 [78]. Emissions of Non-Methane Volatile Organic Compounds (NMVOCs), particulate matter ($PM_{2.5}$ and PM_{10}), organic carbon (OC), black carbon (BC), carbon monoxide (CO), NO_x, and SO_2 at 0.32° × 0.32° spatial resolution are adopted from the SMoG-India V1 2015 emissions inventory [31,79], while the remaining emissions are adopted from EDGARv6 [80]. To assess projected changes in nitrogen deposition, a Future Emission Scenario simulation for the year 2030 (FES-2030) is performed by increasing NH_3 and NO_x emissions by 1.6% and 33% respectively, while maintaining the same model physics and chemistry configuration. These emission adjustments are based on the ECLIPSE V4 scenario [70,81]for India, which incorporates FAO agricultural projections [71] and IEA energy outlooks [82] to represent future conditions. SI-Table S5 shows the NH_3 and NO_x contribution from various emissions sectors over India for BS-2015 and FES-2030 scenarios. Figure5 shows the total NH_3 over the simulation domain with total NH_3 emissions of 6.7 Tg a^{-1} over India.

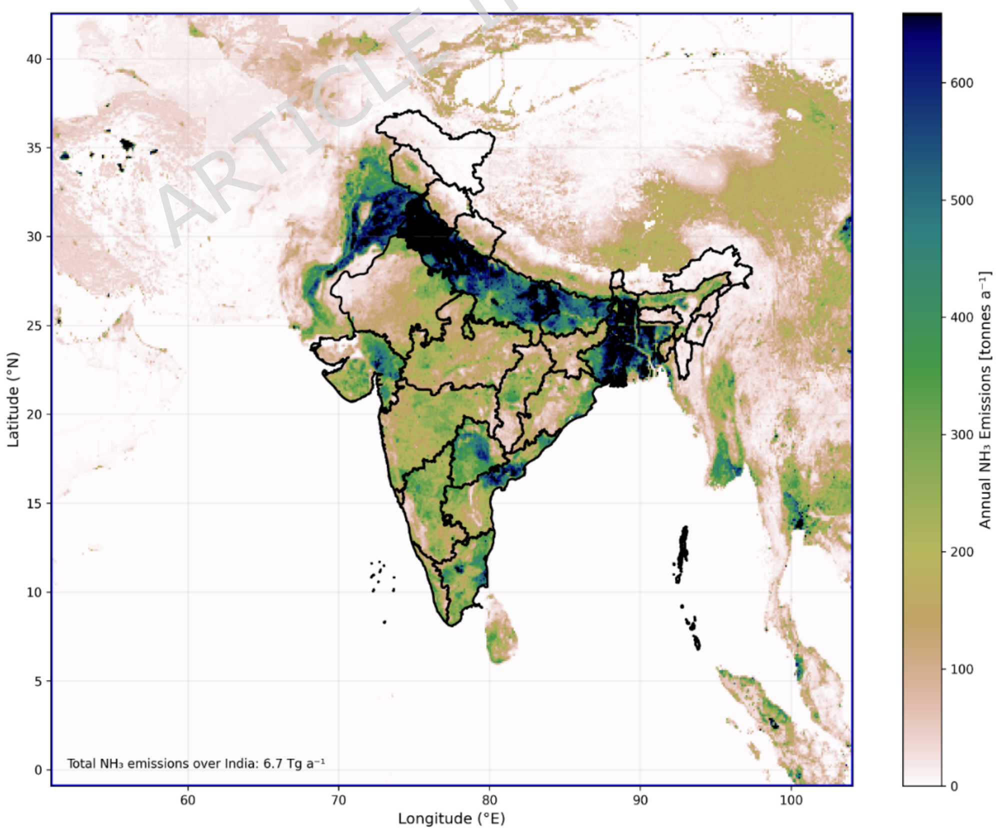

Figure5: Total NH_3 emissions over India (tonnes yr^{-1}) and the computational domain employed in WRF-Chem simulations at a resolution of 0.32° × 0.32° for the year 2015.

Biogenic emissions are calculated online using the Model of Emissions of Gases and Aerosols from Nature (MEGAN v2.1) [83]. Mineral dust emissions are represented using the GOCART dust emission scheme coupled with the MOSAIC aerosol module [84]. Emissions from open biomass burning are taken from the Fire INventory from NCAR (FINNv1.5), and the daily emission fluxes are vertically distributed within the model using the plume-rise parameterization of Freitas et al. (2007) [85]. Chemical initial and lateral boundary conditions are provided by global MOZART-4 simulations, whereas meteorological initial and boundary conditions are obtained from the fifth-generation ECMWF atmospheric reanalysis (ERA5) dataset at 6-hourly intervals. To limit the buildup of meteorological uncertainties, the model is reinitialized every five days, while chemical fields are continuously carried forward across consecutive simulation cycles. This configuration represents the Baseline Simulation for the year 2015 (BS-2015).

Model details

We employ the Weather Research and Forecasting model coupled with chemistry (WRF-Chem, version 4.2.2), which incorporates detailed HCl (hydrogen chloride) and reactive chlorine (Cl) chemistry, important for accurately representing atmospheric processes over India [14]. The chemical mechanism applied here improves the representation of gas-to-particle conversion processes. WRF-Chem enables a fully coupled treatment of emissions, transport, dry and wet deposition, photolysis, radiation, turbulent mixing, and chemical transformation of gases and aerosols in conjunction with meteorological fields [86,87]. Dry deposition is calculated using the resistance-in-series scheme [88], while wet deposition includes both in-cloud (rainout) and below-cloud (washout) scavenging processes for gases and aerosols [89,90]. The simulations are performed at a horizontal grid spacing of 0.32° × 0.32° over the domain 0–45°N and 50–110°E, as illustrated in Figure5. A total of 47 vertical levels are employed, with the model top located at 10 hPa. The physical parameterization schemes applied in this study are listed in SI-Table S6.

The gas-phase chemical reactions in the model are represented using the Model for Ozone and Related Chemical Tracers (MOZART-4) mechanism [91,92]. The aerosol processes implemented within the model is the Model for Simulating Aerosol Interactions and Chemistry (MOSAIC) [93] with four size-resolved bins, such that particle formation, growth, and removal were simulated via nucleation, condensation, coagulation, and dry and wet deposition, along with aerosol-phase [14].

Satellite datasets

Ammonia total column densities (molecules cm^{-2}) are derived from the Level-2 IASI METOP-B product, while tropospheric NO_2 column densities are obtained from the Level-3 daily gridded OMI product available through the NASA Giovanni portal and averaged over the January–August 2015 period [55,94,95]. For NH_3, only morning overpasses (AMPM = 0) satisfying the recommended quality criteria (prefilter = 1, postfilter = 1, and cloud coverage <10%) are used. The filtered NH_3 retrievals are regridded to a 0.3° × 0.3° spatial resolution [82]. Satellite observations of NH_3 and NO_2 are used to evaluate the WRF-Chem simulations for the January–August 2015 period. Corresponding WRF-Chem column densities are calculated by vertically integrating the simulated mixing ratios over the model layers using pressure thickness and are subsequently averaged over the same period. Model performance is evaluated using the correlation coefficient and NMB.

N deposition estimation

The simulated depositions composes of a broad suite of N compounds, including reduced N (RDN or NHx = NH_3 + NH_4^+) and oxidized N (OXY or NO_y), which comprise of NO, NO_2, Nitric acid (HNO_3), peroxynitric acid (HNO_4), and NO_3 radicals. NH_3 and its particulate counterpart NH_4^+ are explicitly treated, enabling the evaluation of gas-to-particle partitioning processes [67,96]. The oxidized N species NO, NO_2, HNO_3, HNO_4, and NO_3 are critical for secondary aerosol formation and atmospheric oxidation capacity. The total N deposition estimated is the sum of all the N*r* species (NO_y + NH_x).

Critical Load exceedance for various ecosystems

The CL values for ecosystems like alpine/sub-alpine/tundra, desert, mangroves/wetlands, evergreen, semi-evergreen, tropical/subtropical forests, deciduous forests have been estimated by performing long term experiments and documented well in China [19], Europe [68] and USA [20]. The detailed review about the various CL studies carried out in China, Europe and USA for the various ecosystem type and the behaviours of sensitive species is tabulated in Shende et al. (2026) [32].

Table1: CL values (kg-N ha^{-1} a^{-1}) prescribed by various China, Europe and USA.

Type of ecosystem	Critical load exceedance (kg-N/ha/a)		
	China[19]	**Europe**[21]	**USA**[20]
Alpine or Sub-Alpine	15 -30	5-15	4-10
Desert	15		3 - 8.4
Mangrove			10 - 15
Evergreen / Semi-evergreen	30 - 70		4 - 7 (Lichens)
			15 (mixed forest)
Tropical or sub-tropical deciduous	30 - 70		15

the orange colour blank cells represent that the CL values for the particular ecosystem is not available by that country

The CL values across China, Europe and USA reveals a significant variations due to the ecosystem sensitivity, atmospheric conditions and the methodological approaches [69]. For alpine/sub-alpine/tundra ecosystems, are vulnerable due to lower N retention rates and shorter growing seasons with CL ranging from 4 kg-N ha^{-1} a^{-1} - 10 kg-N ha^{-1} a^{-1} in USA, 5 kg-N ha^{-1} a^{-1} – 15 kg-N ha^{-1} a^{-1} in Europe and 15 kg-N ha^{-1} a^{-1} – 30 kg-N ha^{-1} a^{-1} in China. Desert/arid ecosystems demonstrate higher regional differentiation with N loading and the CL values defined by USA [3 kg-N ha^{-1} a^{-1} – 8.4 kg-N ha^{-1} a^{-1}] and China [15 kg-N ha^{-1} a^{-1}]. The lower CL (for example : the study performed at Joshua Tree NP, USA) values reflects the sensitivity of these N-limiting area where any N deposition can trigger the growth of invasive species and alter the biodiversity with-in the region [97,98]. For the forest ecosystems like deciduous and evergreen China reported higher CL [30 kg-N ha^{-1} a^{-1} - 70 kg-N ha^{-1} a^{-1}] than USA [15 kg-N ha^{-1} a^{-1}] . The CL varies with respect to the behaviours of the sensitive species to the specific N dose [20,99]. The sensitive species like lichens in the evergreen forests of USA had a tolerance limit of 4 kg-N ha^{-1} a^{-1} - 7 kg-N ha^{-1} a^{-1} whereas mixed forest had CL of 15 kg-N ha^{-1} a^{-1} [20]. A change or replacement in the community composition [19] is commonly observed in evergreen ecosystems along with NO_3^- leaching [20]. The mangrove ecosystem usually responses with increase in the grass cover and rise in the mycorrhizal fungi community with-in the region. The CL defined for this sensitive zone is

10 kg-N ha^{-1} a^{-1} - 15 kg-N ha^{-1} a^{-1} for the coastal scrubs of Mediterranean California, USA. In the present study, we have critically reviewed the CL values for individual ecosystems and have taken them into consideration as was earlier performed in Shende et al. (2026) [32]. A proper consideration of the natural climatic conditions like altitude, temperature and precipitation in these ecosystems from different countries is also taken into account for comparing the CL values for the Indian NPs [32]. Currently we have not taken the soil characteristics and ecosystem processes into consideration as it would go beyond the scope of the present work. Irrespective of this, the study draws focuses on the potential requirement of the long-term assessment of the N loading and understand the N budget and its deposition processes with-in the sensitive zones of India [32,43]. Table1 presents the range of CL exceedance defined by these three countries and will be considered in the present study.

Data availability: The datasets generated during and/or analysed during the study are available in the Supporting Information (SI). Satellite data for NH_3 is available at https://iasi.aeris-data.fr/nh3/ while NO_X is available at https://giovanni.gsfc.nasa.gov/giovanni/. The model output data generated and/or analyzed during the current study are available from the corresponding author upon reasonable request.

References

1. Galloway, J. N. *et al.* Nitrogen Cycles: Past, Present, and Future. *Biogeochemistry* **70**, 153–226, (2004).

2. ERISMAN, J. W. *et al.* The Nitrogen Cascade. *Bioscience* **53**, 341 (2006).

3. Dentener, F. J. *et al.* Nitrogen and Sulfur Deposition on Regional and Global Scales: A Multi-Model Evaluation. *Global Biogeochem. Cycles* 1–20, (2006) doi:10.1029/2005GB002672.

4. Reay, D. S., Dentener, F., Smith, P., Grace, J. & Feely, R. A. Global Nitrogen Deposition and Carbon Sinks. *Nat. Geosci* **1**, 430–437, (2008).

5. Thomas, R. M. *et al.* An Automated Analyzer to Measure Surface-Atmosphere Exchange Fluxes of Water Soluble Inorganic Aerosol Compounds and Reactive Trace Gases. *Environ. Sci. \& Technol.* **43**, 1412–1418 (2009).

6. Guo, J. H. *et al.* Significant Acidification in Major Chinese Croplands. *Science (80-.).* **327**, 1008–1010, (2010).

7. Stevens, C. J. How Long Do Ecosystems Take to Recover from Atmospheric Nitrogen Deposition? *Biol. Conserv.* **200**, 160–167, (2016).

8. Stevens, C. J. *et al.* The Impact of Nitrogen Deposition on Acid Grasslands in the Atlantic Region of Europe. *Env. Pollut* **159**, 2243–2250, (2011).

9. Liu, L. & Greaver, T. L. A Review of Nitrogen Enrichment Effects on Three Biogenic GHGs: The CO2 Sink May Be Largely Offset by Stimulated N2O and CH4 Emission. *Ecol Lett* **12**, 1103–1117, (2009).

10. Bowman, W. D., Cleveland, C. C., Halada, L., Hresko, J. & Baron, J. S. Negative Impact of Nitrogen Deposition on Soil Buffering Capacity. *Nat. Geosci* **1**, 767–770 (2008).

11. Bobbink, R. *et al. Global Assessment of Nitrogen Deposition Effects on Terrestrial Plant Diversity: A Synthesis*. vol. 20 (A Publication of the Ecological Society of America, Ecological Applications, 2010).

12. Richter, A., Burrows, J. P., Nüß, H., Granier, C. & Niemeier, U. Increase in Tropospheric Nitrogen Dioxide over China Observed from Space. *Nature* **437**, 129–132, (2005).

13. Pawar, P. V. *et al.* Analysis of atmospheric ammonia over South and East Asia based on the MOZART-4 model and its comparison with satellite and surface observations. *Atmos. Chem. Phys.* **21**, 6389–6409 (2021).

14. Pawar, P. V *et al.* Chloride (HCl/Cl-) dominates inorganic aerosol formation from ammonia in the Indo-Gangetic Plain during winter: modeling and comparison with observations. *Atmos. Chem. Phys.* **23**, 41–59 (2023).

15. Bauer, S. E. *et al.* Nitrate Aerosols Today and in 2030: A Global Simulation Including Aerosols and Tropospheric Ozone. *Atmos. Chem. Phys.* **7**, 5043–5059, (2007).

16. Li, M. *et al.* Persistent Growth of Anthropogenic Non-Methane Volatile Organic Compound (NMVOC) Emissions in China during 1990–2017: Drivers, Speciation and Ozone Formation Potential. *Atmos. Chem. Phys.* **19**, 8897–8913, (2019).

17. Sutton, M.A., Howard, C. . *The European Nitrogen Assessment: Sources, Effects and Policy Perspectives*. (Cambridge, Sutton, M.A., Howard, C.M, 2011).

18. Ellis, R. A. *et al.* Present and Future Nitrogen Deposition to National Parks in the United States: Critical Load Exceedances. *Atmos. Chem. Phys.* **13**, 9083–9095, (2013).

19. Liu, X. *et al.* Nitrogen Deposition and Its Ecological Impact in China: An Overview. *Environ. Pollut.* **159**, 2251–2264, (2011).

20. Pardo, L. H. *et al.* Effects of Nitrogen Deposition and Empirical Nitrogen Critical Loads for Ecoregions of the United States. *Ecol. Appl.* **21**, 3049–3082, (2011).

21. Bowman, W. D., Gartner, J. R., Holland, K. & Wiedermann, M. Nitrogen Critical Loads for Alpine Vegetation and Terrestrial Ecosystem Response: Are We There Yet? *Ecol Appl* **16**, 1183–1193, (2006).

22. Pandey, R., Gupta, M., Sachdeva, P., Singh, A. & Sugand, S. Biodiversity Conservation in India: Mapping Key Sources and Quantum of Funds. at NIPFP Working Paper 311

(2020).

23. *ENVIS List of National Parks*. https://wii.gov.in/envis (2020).

24. UNDP, S. & U.-W. (2021). Creating a Nature Positive Future: The Contribution of Protected Areas and Other Effective Area-Based Conservation Measures. at (2021).

25. PIB New High-Performance Gas Sensor Can Monitor Low Level Nitrogen Oxides Pollution. at https://www.pib.gov.in/PressReleasePage.aspx?PRID=2051321&reg=48&lang=2 (2024).

26. Yang, A. *et al.* Policies to Combat Nitrogen Pollution in South Asia: Gaps and Opportunities. *Environ. Res. Lett.* **17**, (2022).

27. Sutton, M. A. *et al.* 2 - The Indian Nitrogen Challenge in a Global Perspective. in *The Indian Nitrogen Assessment* (eds. Abrol, Y. P. et al.) 9–28 (Elsevier, 2017). doi:https://doi.org/10.1016/B978-0-12-811836-8.00002-1.

28. Kulshrestha, U. Assessment of Atmospheric Emissions and Deposition of Major Nr Species in Indian Region. in *The Indian Nitrogen Assessment* (ed. Y P Abrol and T K Adhya) (Elsevier, Eds, 2017).

29. Welfare, P. I. B. F. Amrit Kaal: Empowering India's Farmers Through Strategic Fertilizer Policy. at https://static.pib.gov.in/WriteReadData/specificdocs/documents/2025/aug/doc202583598601.pdf (2025).

30. Wang, T. *et al.* Why is the Indo-Gangetic Plain the region with the largest NH3column in the globe during pre-monsoon and monsoon seasons? *Atmos. Chem. Phys.* **20**, 8727–8736 (2020).

31. Pandey, A., Sadavarte, P., Rao, A. & Venkataraman, C. Trends in Multi-Pollutant Emissions from a Technology-Linked Inventory for India: II. *Resid. Agric. Informal Ind. Sect. Atmos. Environ.* **99**, 341–352, (2014).

32. Shende, P., Meena, V. K. & Qureshi, A. Present and Future Atmospheric Nitrogen Deposition and Ecological Critical Load Exceedances in National Parks of India. *ACS EST Air* **3**, 428–436, (2026).

33. Rengarajan, R., Bikkina, S. & Sarin, M. M. Atmospheric Deposition of Reactive Nitrogen over Continental Sites and Oceanic Regions of India: A Review. in *Syposium proceedings: 5th International nitrogen conference* (2010).

34. Singh, A. K. & Mondal, G. C. Chemical Characterization of Wet Precipitation Events and Deposition of Pollutants in Coal Mining Region, India. *J Atmos Chem* **59**, 1–23, (2008).

35. Chandra Mouli, P., Venkata Mohan, S. & Jayarama Reddy, S. A Study on Major Inorganic Ion Composition of Atmospheric Aerosols at Tirupati. *J. Hazard. Mater.* **96**, 217–228, (2003).

36. Parashar, D. C., Kulshrestha, U. C. & Jain, M. Precipitation and Aerosol Studies in India. *Env. Monit Assess* **66**, 47–61, (2001).

37. Das, R., Das, S. N. & Misra, V. N. Chemical Composition of Rainwater and Dustfall at Bhubaneswar in the East Coast of India. *Atmos. Environ.* **39**, 5908–5916, (2005).

38. Satsangi, G. S., Lawrence, A. J., Lakhani, A. & Taneja, A. Assessment of the Potential for Soil Acidification in North India Using the Critical Load Approach and Locally Derived Data for Acidic and Basic Inputs. *Chemosphere* **53**, 1011–1021, (2003).

39. Momin, G. A. *et al.* Study of Chemical Composition of Rainwater at an Urban (Pune) and a Rural (Sinhagad) Location in India. *J. Geophys. Res. Atmos.* **110**, (2005).

40. Ravichandran, C. & Padmanabhamurty, B. Acid Precipitation in Delhi, India. *Atmos. Environ.* **28**, 2291–2297, (1994).

41. Kulshrestha, U. C., Sarkar, A. K., Srivastava, S. S. & Parashar, D. C. Investigation into Atmospheric Deposition through Precipitation Studies at New Delhi (India). *Atmos. Environ.* **30**, 4149–4154, (1996).

42. Singh, Ak. *et al.* Precipitation Chemistry and Occurrence of Acid Rain Over Dhanbad, Coal City of India. *Env. Monit Assess* **125**, 99–110, (2007).

43. Gautam, M. K., Tripathi, A. K. & Manhas, R. K. Assessment of Critical Loads in Tropical Sal (Shorea Robusta Gaertn. F.) Forests of Doon Valley Himalayas, India. *Water Air Soil Pollut* **218**, 235–264, (2011).

44. Rao, P. S. P., Safai, P. D., Budhavant, K. & Soni, V. K. *Wet Deposition of Nitrogen at Different Locations in India. Nitrogen Deposition, Critical Loads and Biodiversity* (Springer, Dordrecht, S, 2014). doi:10.1007/978-94-007-7939-6_13.

45. *Nitrogen Deposition, Critical Loads and Biodiversity*. (Springer, 2014). doi:10.1007/978-94-007-7939-6.

46. Sharma, D. & Kulshrestha, U. C. Chemistry of Atmospheric Dust and Critical Load Assessment in Delhi Region (India). *Chem. Ecol.* **34**, 470–481, (2018).

47. Kulshrestha, U. Gaps in Nitrogen Deposition Measurements in South Asia. *Curr. World Environ.* **17**, 284–288, (2022).

48. Pillai, A. G. *et al.* Studies of Wet Deposition and Dustfall at Pune, India. *Water, Air, Soil Pollut.* **130**, 475–480, (2001).

49. Rastogi, N. & Sarin, M. Atmospheric Abundances of Nitrogen Species in Rain and Aerosols Over a Semi-Arid Region: Sources and Deposition Fluxes. *Aerosol Air Qual. Res* **6**, 406–417, (2006).

50. Kulshrestha, U. C., Kulshrestha, M. J., Sekar, R., Sastry, G. S. R. & Vairamani, M. Chemical Characteristics of Rainwater at an Urban Site of South-Central India. *Atmos. Environ.* **37**, 3019–3026, (2003).

51. Sutton, M. A. *et al.* The Indian nitrogen assessment : sources of reactive nitrogen, environmental and climate effects, management options, and policies. in *The Indian Nitrogen Assessment* (eds. Abrol, Y. P. et al.) 9–25 (Elsevier, 2017). doi:https://doi.org/10.1016/B978-0-12-811836-8.01002-8.

52. Abrol, Y. & Adhya, T. Technical Summary. *Indian Nitrogen Assess.* 1–5, (2017) doi:10.1016/B978-0-12-811836-8.00001-X.

53. Tomlinson, S. J. *et al.* A Framework for Gridded Estimates of Ammonia Emissions from Agriculture in South Asia. *Earth Syst. Sci. Data Discuss.* 1–31, (2025) doi:10.5194/essd-2025-75.

54. Abrol, Y. P. *et al. The Indian Nitrogen Assessment : Sources of Reactive Nitrogen, Environmental and Climate Effects, Management Options, and Policies*.

55. Ghude, S. D. *et al.* Satellite constraints of nitrogen oxide (NOx) emissions from India based on OMI observations and WRF-Chem simulations. *Geophys. Res. Lett.* **40**, 423–428 (2013).

56. Clarisse, L., Clerbaux, C., Dentener, F., Hurtmans, D. & Coheur, P. F. Global ammonia distribution derived from infrared satellite observations. *Nat. Geosci.* **2**, 479–483 (2009).

57. Zhang, X. F. Atmospheric Nitrogen Wet Deposition and Its Effects on Wetland Water Environment of Shanghai Area. *Chinese J. Appl. Ecol.* **17**, 1099–1102 (2006).

58. Gotelli, N. J., Ellison, A. M. N. I. T. R. O. G. E. N. D. E. P. O. S. I. T. I. O. N. & PLANT, E. X. T. I. N. C. T. I. O. N. R. I. S. K. I. N. T. H. E. N. O. R. T. H. E. R. N. P. I. T. C. H. E. R. NITROGEN DEPOSITION AND EXTINCTION RISK IN THE NORTHERN PITCHER PLANT, SARRACENIA PURPUREA. *Ecology* **83**, 2758–2765, (2002).

59. Gotelli, N. J. & Ellison, A. M. FORECASTING EXTINCTION RISK WITH NONSTATIONARY MATRIX MODELS. *Ecol. Appl.* **16**, 51–61 (2006).

60. Latimer, J. S. & Rego, S. A. Empirical Relationship between Eelgrass Extent and Predicted Watershed-Derived Nitrogen Loading for Shallow New England Estuaries. *Estuar. Coast. Shelf Sci.* **90**, 231–240, (2010).

61. Ou, M. S. & Lü, S. H. Efects of Diferent Inorganic Nitrogen Sources on the Growth of Prorocentrum Donghaiense. *Ecol. Sci.* **25**, 28–31.

62. Zhuoping, C., Weiwei, H. & Duan, S. Cell Proliferation of Phaeocystis Globasa, a Red Tide Causative Marine Microalga in Various Phosphorus (P)-and Nitrogen (N) - Replete Conditions. *Ecol. Environ. Sci.* **8**, 447–452 (2009).

63. Baron, J. S. Hindcasting Nitrogen Deposition To Determine An Ecological Critical Load. *Ecol. Appl. - Wiley Online Libr.* **16**, 433–439 (2006).

64. Caffrey, J. M., Murrell, M. C., Wigand, C. & McKinney, R. Effect of Nutrient Loading on Biogeochemical and Microbial Processes in a New England Salt Marsh. *Biogeochemistry* **82**, 251–264, (2007).

65. Wigand, C., McKinney, R., Charpentier, M. A., Chintala, M. M. & Thursby, G. B. Relationships of Nitrogen Loadings, Residential Development, and Physical Characteristics with Plant Structure in New England Salt Marshes. *Estuaries* **26**, 1494–1504, (2003).

66. Aber, J. D. *et al.* Is Nitrogen Deposition Altering the Nitrogen Status of Northeastern Forests? *Bioscience* **53**, 375–389, (2003).

67. Finlaysons-Pitts B.J.; Pitts Jr., J. N. Chemistry of the Upper and Lower Atmosphere- Theory. *Exp. Appl.* (2000).

68. Bobbink, R. *et al.* Empirical nitrogen critical loads for natural and semi-natural ecosystems: 2002 update. *Empir. Crit. loads …* 1–128 (2002).

69. Lu, X. *et al.* Simulated Effects of Nitrogen Saturation on the Global Carbon Budget Using the IBIS Model. *Sci Rep* **6**, 39173 (2016).

70. Klimont, Z. *et al.* Projections of SO2, NOx and Carbonaceous Aerosols Emissions in Asia. *Tellus B Chem. Phys. Meteorol.* 602–617 (2009).

71. Alexandratos, N. & Bruinsma, J. WORLD AGRICULTURE TOWARDS 2030 / 2050 The 2012 Revision. Global Perspective Studies Team, FAO Agricultural Development Economics Division. ESA Working Paper No. 12-03. http://www.fao.org/docrep/016/ap106e/ap106e.pdf (2012).

72. Klimont, Z. *et al.* Global gridded anthropogenic emissions of air pollutants and methane for the period 1990-2050. at https://doi.org/10.5281/zenodo.14748815 (2025).

73. Sutton, M. A. *et al.* Towards a climate-dependent paradigm of ammonia emission and deposition. *Philos. Trans. R. Soc. B Biol. Sci.* **368**, 20130166–20130166 (2013).

74. van der Graaf, S. C., Dammers, E., Schaap, M. & Erisman, J. W. Technical note: How are \chem{NH_3} dry deposition estimates affected by combining the LOTOS-EUROS model with IASI-\chem{NH_3} satellite observations? *Atmos. Chem. Phys.* **18**, 13173–13196 (2018).

75. Hu, C. *et al.* Modeling the Sources and Transport Processes During Extreme Ammonia Episodes in the U.S. Corn Belt. *J. Geophys. Res. Atmos.* **125**, e2019JD031207 (2020).

76. Feng, S. *et al.* The impact of emissions controls on atmospheric nitrogen inputs to Chinese river basins highlights the urgency of ammonia abatement. *Sci. Adv.* **10**, eadp2558 (2024).

77. Kang, J. *et al.* Ammonia mitigation campaign with smallholder farmers improves air quality while ensuring high cereal production. *Nat. Food* **4**, 751–761 (2023).

78. Zhang, B. *et al.* Global Emissions of Hydrogen Chloride and Particulate Chloride from Continental Sources. *Environ. Sci. Technol* **56**, 3894–3904, (2022).

79. Venkataraman, C. *et al.* Source influence on emission pathways and ambient PM$_{2.5}$ pollution over India (2015--2050). *Atmos. Chem. Phys.* **18**, 8017–8039 (2018).

80. Crippa, M. *et al.* Global Anthropogenic Emissions in Urban Areas: Patterns, Trends, and Challenges. *Environ. Res. Lett* **16**, 074033 (2021).

81. Amann, M., Klimont, Z. & Wagner, F. Regional and Global Emissions of Air Pollutants: Recent Trends and Future Scenarios. *Annu. Rev. Environ. Resour.* **38**, 31–55, (2013).

82. *World Energy Outlook 2011*. https://www.iea.org/reports/world-energy-outlook-2011 (2011).

83. Guenther, A. B. *et al.* The Model of Emissions of Gases and Aerosols from Nature Version 2.1 (MEGAN2.1): An Extended and Updated Framework for Modeling Biogenic Emissions. *Geosci. Model Dev.* **5**, 1471–1492, (2012).

84. Ginoux, P., Chin, M., Tegen, I., Goddard, T. & In-, G. Sources and distribution of dust aerosols simulated with the GOCART model. *J. Geophys. Res.* **106**, 20255–20273 (2001).

85. Freitas, S. R. *et al.* Including the sub-grid scale plume rise of vegetation fires in low resolution atmospheric transport models. *Atmos. Chem. Phys.* **7**, 3385–3398 (2007).

86. Li, W. *et al.* On the Contribution of Atmospheric Reactive Nitrogen Deposition to Nitrogen Burden in a Eutrophic Lake in Eastern China. *Water Res.* **268**, 122597 (2025).

87. Luo, G. & Yu, F. Simulation of Particle Formation and Number Concentration over the Eastern United States with the WRF-Chem + APM Model. *Atmos. Chem. Phys.* **11**, 11521–11533, (2011).

88. Wesely, M. L. Parameterization of surface resistances to gaseous dry deposition in regional-scale numerical models. *Atmos. Environ.* **23**, 1293–1304 (1989).

89. Grell, G. A. *et al.* Fully Coupled "Online" Chemistry within the WRF Model. *Atmos. Environ.* **39**, 6957–6975, (2005).

90. Grell, G. A. & Freitas, S. R. A Scale and Aerosol Aware Stochastic Convective Parameterization for Weather and Air Quality Modeling. *Atmos. Chem. Phys.* **14**, 5233–5250, (2014).

91. Emmons, L. K. *et al.* Description and evaluation of the Model for Ozone and Related chemical Tracers, version 4 (MOZART-4). *Geosci. Model Dev.* **3**, 43–67 (2010).

92. Knote, C., Hodzic, A. & Jimenez, J. L. The effect of dry and wet deposition of condensable vapors on secondary organic aerosols concentrations over the continental US. *Atmos. Chem. Phys.* **15**, 1–18 (2015).

93. Zaveri, R. A., Easter, R. C., Fast, J. D. & Peters, L. K. Model for Simulating Aerosol Interactions and Chemistry (MOSAIC). *J. Geophys. Res. Atmos.* **113**, 1–29 (2008).

94. Van Damme, M. *et al.* Industrial and agricultural ammonia point sources exposed. *Nature* **564**, 99–103 (2018).

95. Lamsal, L. N. *et al.* Ozone Monitoring Instrument (OMI) Aura nitrogen dioxide standard product version 4.0 with improved surface and cloud treatments. *Atmos. Meas. Tech.* **14**, 455–479 (2021).

96. Seinfeld, J.H. and Pandis, S. N. *Atmospheric Chemistry and Physics: From Air Pollution to Climate Change*. (New York., 2016).

97. Báez, S., Fargione, J., Moore, D. I., Collins, S. L. & Gosz, J. R. Atmospheric Nitrogen Deposition in the Northern Chihuahuan Desert: Temporal Trends and Potential Consequences. *J. Arid Environ.* **68**, 640–651, (2007).

98. Allen, E. B., Rao, L. E., Steers, R. J., Bytnerowicz, A. & Fenn, M. E. Impacts of Atmospheric Nitrogen Deposition on Vegetation and Soil at Joshua Tree National Park. *Atmos. Nitrogen Depos.* 27 (2009).

99. Bobbink, R. *et al.* Effects and Empirical Critical Loads of Nitrogen for Europe. in *Critical Loads and Dynamic Risk Assessments: Nitrogen, Acidity and Metals in Terrestrial and Aquatic Ecosystems* (eds. Vries, W., Hettelingh, J.-P. & Posch, M.) 85–127 (Dordrecht, Springer Netherlands, 2015).

Acknowledgments

The authors declare no competing interests, financial or otherwise, that could have influenced the research reported in this study. The authors are thankful to the Director, Indian Institute of Tropical Meteorology (IITM), Pune. We would like to acknowledge high-performance computing support from Pratyush and ARKA provided by the IITM. The authors are grateful to UK Research and Innovation for their continuous support and guidance, and for providing the ammonia (NH_3) emission input data used in this study, conducted under the South Asian Nitrogen Hub (SANH). The authors are also grateful to Dr. Asif Qureshi for sharing the GOES-Chem N deposition values for model comparison.

Author contributions

All authors contributed to the conception and design of the study. S.D.G. and P.V.P. conceived and initiated the study. M.A.S. contributed to the development of the NH_3 emission inventory and reviewed and edited the manuscript. P.V.P. performed the model simulations. P.S. processed and analyzed the simulation data, prepared the visualizations, and wrote and edited the manuscript. All authors reviewed and approved the final manuscript. The first draft of manuscript was written by P.S. and all authors commented on the previous versions of the manuscript. All the authors read and approved the final manuscript.

Competing interest: The authors declare no competing financial interest.

Funding

The author(s) received no financial support for the research, authorship, and/or publication of this article.

Figure legends

Figure1: Comparison of model results with ground-based observations reported in studies conducted across India.

Figure2: Comparison of simulated and satellite-derived total (a) NH_3 and (b) NO_2 column (molecules cm^2) over India.

Figure3: Spatial oxidized, reduced and total N deposition for the BS-2015 and FES-2030 over India.

Figure4: Total N deposition (kg-N ha^{-1} a^{-1}) in ecologically sensitive zones of India under the BS-2015 (blue colour bar) and FES-2030 (red colour bar) containing the minimum and the maximum total N deposition for specific ecosystems of India along with the NP name. The background blue colour represents the USA CL limits, green (in the alpine region) represents the Europe CL limits and the red colour band is the China CL limits.

Figure5: Total NH_3 emissions over India (tonnes yr^{-1}) and the computational domain employed in WRF-Chem simulations at a resolution of 0.32° × 0.32° for the year 2015.

Tables

Table1: CL values (kg-N ha^{-1} a^{-1}) prescribed by various China, Europe and USA.

Type of ecosystem	Critical load exceedance (kg-N/ha/a)		
	China[19]	**Europe**[21]	**USA**[20]
Alpine or Sub-Alpine	15 -30	5-15	4-10
Desert	15		3 - 8.4
Mangrove			10 - 15
Evergreen / Semi-evergreen	30 - 70		4 - 7 (Lichens)
			15 (mixed forest)
Tropical or sub-tropical deciduous	30 - 70		15
the orange colour blank cells represent that the CL values for the particular ecosystem is not available by that country			